

Durham Research Online

Deposited in DRO:

12 April 2013

Version of attached file:

Accepted Version

Peer-review status of attached file:

Peer-reviewed

Citation for published item:

Ishikawa, A. and Pearson, D.G. and Dale, C.W. (2011) 'Ancient Os isotope signatures from the Ontong Java Plateau lithosphere : tracing lithospheric accretion history.', *Earth and planetary science letters.*, 301 (1-2). pp. 159-170.

Further information on publisher's website:

<http://dx.doi.org/doi:10.1016/j.epsl.2010.10.034>

Publisher's copyright statement:

NOTICE: this is the author's version of a work that was accepted for publication in *Earth and planetary science letters*. Changes resulting from the publishing process, such as peer review, editing, corrections, structural formatting, and other quality control mechanisms may not be reflected in this document. Changes may have been made to this work since it was submitted for publication. A definitive version was subsequently published in *Earth and planetary science letters*, 301 (1-2), 2011, 10.1016/j.epsl.2010.10.034

Additional information:

Use policy

The full-text may be used and/or reproduced, and given to third parties in any format or medium, without prior permission or charge, for personal research or study, educational, or not-for-profit purposes provided that:

- a full bibliographic reference is made to the original source
- a [link](#) is made to the metadata record in DRO
- the full-text is not changed in any way

The full-text must not be sold in any format or medium without the formal permission of the copyright holders.

Please consult the [full DRO policy](#) for further details.

**Ancient Os isotope signatures from the Ontong Java
Plateau lithosphere: tracing lithospheric accretion
history**

Akira Ishikawa^{a,b,*}, D. Graham Pearson^{a,c}, Christopher W. Dale^a

^a*Arthur Holmes Isotope Geology Laboratory, Department of Earth
Sciences, Durham University, South Road, Durham, DH1 3LE, UK*

^b*Institute for Research on Earth Evolution (IFREE), Japan Agency for
Marine-Earth Science and Technology (JAMSTEC), 2-15, Natsushima-cho,
Yokosuka, Japan*

^c*Department of Earth and Atmospheric Sciences, University of Alberta,
1-26 Earth Sciences Building, Edmonton AB, T6G 2E3, Canada.*

*Corresponding author

Present address: Department of Earth Science and Astronomy, The University of Tokyo
at Komaba, 3-8-1, Komaba, Meguro, Tokyo, 153-8902, Japan

Phone: +81-3-5454-6364 / E-mail: akr@ea.c.u-tokyo.ac.jp

Submitted to *Earth and Planetary Science Letters*, June 2010

Revised form submitted in October 2010

Body text word count: 6420/ Figures: 8/ Table: 1/References: 70

29 ABSTRACT

30 *In order to better understand the nature and formation of oceanic lithosphere beneath*
31 *the Early Cretaceous Ontong Java Plateau, Re-Os isotopes have been analysed in a*
32 *suite of peridotite xenoliths from Malaita, Solomon Islands. Geological,*
33 *thermobarometric and petrological evidence from previous studies reveal that the*
34 *xenoliths represent virtually the entire thickness of the southern part of subplateau*
35 *lithospheric mantle (<120 km). This study demonstrates that vertical Os isotopic*
36 *variations correlate with compositional variations in a stratified lithosphere. The*
37 *shallowest plateau lithosphere (<85 km) is dominated by fertile lherzolites showing a*
38 *restricted range of $^{187}\text{Os}/^{188}\text{Os}$ (0.1222 to 0.1288), consistent with an origin from ~160*
39 *Ma Pacific lithosphere. In contrast, the basal section of subplateau lithospheric mantle*
40 *(~95-120 km) is enriched in refractory harzburgites with highly unradiogenic*
41 *$^{187}\text{Os}/^{188}\text{Os}$ ratios ranging from 0.1152 to 0.1196, which yield Proterozoic model ages*
42 *of 0.9-1.7 Ga. Although the whole range of Os isotope compositions of Malaita*
43 *peridotites is within the variations seen in modern abyssal peridotites, the contrasting*
44 *isotopic compositions of shallow and deep plateau lithosphere suggest their derivation*
45 *from different mantle reservoirs. We propose that the subplateau lithosphere forms a*
46 *genetically unrelated two-layered structure, comprising shallower, typical oceanic*
47 *lithosphere underpinned by deeper impinged material, which included a component of*
48 *recycled Proterozoic lithosphere. The impingement of residual but chemically*
49 *heterogeneous mantle, mechanically coupled to the recently-formed, thin lithosphere,*
50 *may have a bearing on the anomalous initial uplift and late subsidence history of the*
51 *seismically anomalous plateau root.*

52

53 *Key words: xenoliths; peridotite; Ontong Java Plateau; Re-Os isotopes;*
54 *recycling; mantle plume*

55

1. Introduction

The Early Cretaceous Ontong Java Plateau in the western Pacific is the most voluminous large igneous province on the Earth, with an area of $\sim 2 \times 10^6 \text{ km}^2$ and a maximum crustal thickness of $>30 \text{ km}$ (e.g. Richardson et al., 2000; Miura et al., 2004). Almost the entire plateau is thought to have been generated by massive volcanism in a single episode ca. 122 Ma (Mahoney et al., 1993; Tejada et al., 1996; Parkinson et al., 2002; Tejada et al., 2002), generally attributed to large-scale mantle plume activity. Thus, the nature and origin of the plateau has received widespread interest due to its implications for the dynamics of the Earth's mantle and possible global environmental impact (e.g. Courtillot and Olson, 2007). However, the origin of the Ontong Java Plateau remains contentious as to whether the voluminous magmatism was due to melting of a high-temperature mantle plume. The high-potential mantle temperature ($T_p > 1500 \text{ }^\circ\text{C}$) estimated from the geochemical characteristics of plateau lavas (Fitton and Godard, 2004; Herzberg, 2004) is apparently incompatible with the minor initial uplift (2.5-3.6 km above the surrounding seafloor) and post-eruption subsidence ($1.5 \pm 0.4 \text{ km}$) documented by the submarine eruption of plateau lavas (Roberge et al., 2005). This has led several researchers to propose alternative models which do not invoke plume activity (e.g. Ingle and Coffin, 2004; Korenaga, 2005), but these non-plume hypotheses can not adequately explain lava geochemistry (e.g., Kerr and Mahoney, 2007). Since this discrepancy between geochemical and geophysical approaches likely originates from certain specific assumptions regarding the nature of the source mantle and its consequences for the lithospheric structure, it is crucial to constrain the origin and evolution of the lithospheric mantle underlying the plateau. This will lead to a better understanding of the causal mechanisms of plateau formation, and other large igneous provinces in general.

An important resource for understanding the subplateau lithosphere is the varied

suite of mantle xenoliths found in 34 Ma alnöite intrusions on the Solomon Island of Malaita (e.g. Nixon and Boyd, 1979; Nixon and Neal, 1987). Malaita is located on the uplifted southwestern margin of the Ontong Java Plateau, resulting from its collision against the Solomon arc (Fig. 1). The first contact between the Solomon arc in the overlying Australian Plate and the plateau in the subducting Pacific Plate commenced about 20-25 Ma (Pettersen et al., 1997), suggesting that xenolith entrainment by the host alnöite occurred in an oceanic environment (Fig. 1B). Previous thermobarometry revealed that the xenolith suite, including both peridotites and pyroxenites were equilibrated over a wide range of P - T conditions (770-1340°C, 1.6-3.6 GPa, Nixon and Boyd, 1979; Ishikawa et al., 2004) corresponding to depths of 60-120 km (Fig. 2A), defining a geotherm typical of old oceanic lithosphere. Thus, geological and thermobarometric evidence suggest that the xenoliths represent virtually an entire section of the subplateau lithosphere that is not associated with any known subducting slab or slab-related structures. The lithological structure, reconstructed on the basis of predominant lithologies within different depth intervals, can be interpreted in terms of normal oceanic lithosphere subsequently influenced by the plateau thickening.

Perhaps the most important inference arising from the above petrological reconstruction is that the lower section of subplateau lithosphere may represent melting residues from Ontong Java Plateau magmatism (Ishikawa et al., 2004). This interpretation is largely based on the presence of an intra-lithospheric depleted zone of ~15 km thickness between 85 and 100 km, which is barren of garnet-bearing xenoliths (Fig. 2B). This interval is dominated by highly depleted harzburgites containing olivine with high forsterite content [$\text{Fo} = \text{molar } 100\text{Mg}/(\text{Mg}+\text{Fe}) \sim 92$], and is overlain by a succession of more fertile mantle that has undergone small degrees of melting at a normal seafloor spreading center some 40 Ma before the plateau magmatism (Ishikawa et al., 2005). To generate the refractory residues in a high-pressure environment (~2.5 GPa or more) at the base of pre-existing oceanic lithosphere, ascending mantle would

require a very high- T_p , in excess of 1600°C (Fig. 2A). This constraint appears to conform to a hot-plume hypothesis for the plateau generation.

In order to evaluate whether or not such refractory residues were created by melting in a recently active plume, we carried out a Re-Os isotope study of Malaita peridotite xenoliths covering the spectrum of P - T and lithological variations. The advantage of the Re-Os isotope system is two-fold. Firstly, the vast majority of peridotite xenoliths are subjected to post-crystallization disturbance e.g. mantle metasomatism, infiltration of host alnöite and seawater alteration, precluding the comprehensive identification of primary signatures based on highly incompatible element isotope systems (Neal, 1988; Ishikawa et al., 2005). In contrast, the Re-Os isotope system has a greater potential to identify the primary signatures because of its relative immunity to secondary effects (e.g. Pearson and Wittig, 2008). Secondly, melt depletion significantly lowers the Re/Os ratio of mantle peridotites and retards the ingrowth of ^{187}Os from the decay of ^{187}Re , allowing the timing of melt depletion to be estimated solely from $^{187}\text{Os}/^{188}\text{Os}$ ratios, using the Re-depletion model age (T_{RD}) concept (e.g. Walker et al., 1989). Hence, the Re-Os isotope system is particularly suitable for dating refractory harzburgites and therefore can address the origin of the deep harzburgitic root of the Ontong Java Plateau.

2. Samples and methods

Samples investigated here include spinel lherzolite, spinel harzburgite, garnet-spinel lherzolite and garnet lherzolite (Table 1) from the Malaita alnöite intrusion. Detailed individual sample locations are unavailable because the xenoliths were usually found in dense rain forests and river deposits that precluded accurate location. The classification of rock types, petrographic and major element characteristics of constituent minerals together with their equilibrium conditions have previously been described by Ishikawa et al. (2004). Garnet lherzolites and some spinel harzburgites

belong to a high-temperature (high-T) group, derived from greater depths (>95 km) than the low-temperature (low-T) group (<95 km).

For the most part, mineral chemistry in both peridotite types is consistent with their origin as melting residues, as is most clearly indicated by their high Fo contents (Fig. 2B). In contrast, whole-rock compositions have been variably influenced by metasomatic enrichment and surficial alteration, as documented by their typically high LOI values. The effects of these processes are clearly indicated by the development of texturally equilibrated amphibole (<20 vol%) and serpentine-carbonate replacing olivine. In order to test to what extent the Re-Os isotope system is resistant to such effects, we analysed a range of peridotites including less altered samples - defined as <2.5 wt% loss on ignition (LOI) - along with highly altered samples (>2.5 wt% LOI) selected from the lithological spectrum. Extremely altered samples (>10 wt% LOI) were not analysed.

Xenoliths were sawn and their surfaces ground with corundum paper to remove metal contaminants and alteration. Samples were disaggregated between thick plastic sheets with a rock hammer and then powdered in an agate mill and mortar. Al₂O₃ concentrations were determined by XRF on fused glass beads at Leicester University, UK. Concentration and isotopic measurements for Re-Os were performed at Durham University, UK, using isotope dilution mass spectrometry (NTIMS for Os, ICPMS for Re) after acid digestion in an Anton-Paar High Pressure Asher. Details of the procedure for sample digestion, chemical purification and mass spectrometry were reported in Dale et al. (2009) and references therein. Analyses of 170 pg aliquots of the University of Maryland Os standard solution (UMCP), giving similar signal sizes to sample loads, gave a mean ¹⁸⁷Os/¹⁸⁸Os of 0.11379±14 (2σ_{mean}, n=39) over the period of analysis, in good agreement with a value of 0.113787±7 for 10–100 ng/g aliquots measured on the same instrument in Faraday cup mode (Luguet et al., 2008). Replicate analyses of in-house standard sample (GP13, n=7) yield 0.315±0.006 ppb for Re, 3.97±0.26 ppb for

Os and 0.12604 ± 20 for $^{187}\text{Os}/^{188}\text{Os}$ ratio (errors quoted at $2\sigma_{\text{mean}}$), in good agreement with published values (Pearson et al., 2004; Puchtel et al., 2008, and references therein). Re-Os analyses have been duplicated for 4 samples (Table 1), three of which display good reproducibility for Re and Os concentrations and $^{187}\text{Os}/^{188}\text{Os}$ ratios between duplicates ($<12.5\%$, $<15.5\%$ and $<1\%$ RSD, respectively). In contrast, sample SAS63 shows larger variability in both Re and Os concentrations (95%, 54%, respectively), probably due to the relatively low concentrations in this sample.

3. Results

3.1. Low-temperature peridotites

Whole-rock Al_2O_3 contents of the low-T peridotites vary from 1.0 to 7.3 wt%, indicating a wide range in fertility. There are broad correlations between whole-rock Al_2O_3 and both olivine Fo and spinel Cr-number (Cr#), except for garnet-spinel lherzolites whose spinel Cr#s were increased by subsolidus formation of garnet (Fig. 3). The overall trends are very similar to those observed for the global compilation of oceanic peridotites including abyssal peridotites and xenoliths from ocean islands. This covariation is consistent with an origin as residues of variable degrees of melt depletion. However, it is evident that several samples do not plot on the apparent depletion trends. Two garnet-spinel lherzolites have whole-rock Al_2O_3 contents (7.3 and 6.0 wt%), which are markedly higher than the other lherzolites (2.0-4.9 wt%) or estimates of average depleted MORB mantle (DMM, 3.98 wt% Al_2O_3 ; Workman and Hart, 2005) and primitive upper mantle (PUM, 4.44 wt% Al_2O_3 ; McDonough and Sun, 1995). Such Al_2O_3 enrichment is evident as an overabundance of garnet in the mode (>15 vol%). Two spinel-facies cpx-free peridotites with higher Al_2O_3 contents (2.3 and 3.0 wt%) than the majority of harzburgites (1.0-2.0 wt%), contain high-Cr# spinel (0.61 and 0.62), slightly low-Fo olivine (89.3 and 89.7) and abundant amphibole (14 and 17 vol%). These represent strongly metasomatised samples, which we can use to evaluate

metasomatic effects on Re-Os isotope compositions.

Whole rock Re concentrations in the low-T peridotites vary from 0.003 to 0.92 ppb (Table 1), overlapping the range for abyssal peridotites and peridotite xenoliths from ocean islands (Fig. 4). The majority of low-T peridotites have relatively low Re concentrations (mean 0.18 ppb) compared to the PUM estimate (0.35 ± 0.06 ppb; Becker et al., 2006), consistent with the incompatible behavior of Re during mantle melting. This is also illustrated by the lower Re contents of spinel harzburgites (mean 0.06 ppb) than spinel lherzolites and garnet-spinel lherzolites (mean 0.23 versus 0.22 ppb). However, no clear correlation exists between Re concentrations and the indices of melt extraction discussed above. This may be explained by Re enrichment because several samples (spinel- or garnet-spinel lherzolites) have significantly higher Re than the PUM estimate.

Os concentrations in spinel lherzolites and garnet-spinel lherzolites range from 1.8 to 5.6 ppb and 3.0 to 7.4 ppb, with mean values of 3.9 and 4.3 ppb, respectively, overlapping the range found in other oceanic peridotites (Fig. 4). Mean Os concentrations for the lherzolites are almost identical to the PUM estimate of 3.9 ± 0.5 (Becker et al., 2006), indicating the compatible behavior of Os during mantle melting. Spinel harzburgites, however show a greater variation in Os concentration (0.03-5.8 ppb), with one anomalously high value (13.0 ppb - sample SAS30). Samples with less than 1 ppb Os are limited to highly depleted compositions ($\text{Al}_2\text{O}_3 < 1.5$ wt%; Fo >91), whereas Os concentrations for harzburgites containing low-Fo olivine (<90) are higher than average values of lherzolite and the PUM estimate.

Present-day $^{187}\text{Os}/^{188}\text{Os}$ ratios of the low-T peridotites yield an average ratio of 0.1258 (n=58), and range from 0.1163 to 0.1404 (Table 1, Fig. 5). Most of these values, while overlapping the chondritic range, are significantly less radiogenic than the chondritic average ($^{187}\text{Os}/^{188}\text{Os}=0.1276$, Walker et al., 2002) and PUM ($^{187}\text{Os}/^{188}\text{Os}=0.1296$, Meisel et al., 2001). These values are comparable to those of

abyssal peridotites (mean: $^{187}\text{Os}/^{188}\text{Os}=0.1249$; range: 0.1139-0.1385, $n=125$) and peridotite xenoliths from ocean islands (mean: $^{187}\text{Os}/^{188}\text{Os}=0.1236$; range: 0.1138-0.1383, $n=60$), supporting their derivation from an oceanic setting. When differentiated by rock type, garnet-spinel lherzolites tend to have slightly more radiogenic Os (mean $^{187}\text{Os}/^{188}\text{Os}=0.1276$, $n=16$) than spinel lherzolites (mean $^{187}\text{Os}/^{188}\text{Os}=0.1259$, $n=24$) and spinel harzburgites (mean $^{187}\text{Os}/^{188}\text{Os}=0.1241$, $n=18$). However, such variations cannot be directly attributed to any clear chronological difference as there is a lack of definitive correlation, on a lithological basis, between $^{187}\text{Os}/^{188}\text{Os}$ and $^{187}\text{Re}/^{188}\text{Os}$ or any robust indicators of the degree of melt-depletion such as whole-rock Al_2O_3 , olivine Fo content or spinel Cr# (Figs. 6 and S1 in the Appendix).

Scattering of present-day $^{187}\text{Os}/^{188}\text{Os}$ ratios in spinel harzburgites ($^{187}\text{Os}/^{188}\text{Os}=0.1163$ -0.1339) can be related to the varying effect of ^{187}Re ingrowth due to the large range of $^{187}\text{Re}/^{188}\text{Os}$ ratios from ~ 0.006 to 8.3 (Fig. 6 inset). When the data are corrected for in situ decay of Re since the 122 Ma age of the Ontong Java Plateau magmatism, they can be subdivided into two populations with differing initial $^{187}\text{Os}/^{188}\text{Os}$ ratios. A main group ($n=14$) has $^{187}\text{Os}/^{188}\text{Os}_{122\text{ Ma}}$ of 0.1221 to 0.1247, whereas others ($n=4$) have very unradiogenic $^{187}\text{Os}/^{188}\text{Os}_{122\text{ Ma}}$ ranging from 0.1161 to 0.1171. However, these groups cannot be differentiated on the basis of whole-rock Al_2O_3 and LOI contents, or petrography and mineral chemistry.

3.2. High-temperature peridotites

As with the low-T Malaita peridotites, whole-rock Al_2O_3 contents of the high-T peridotites vary according to rock type and mineral compositions: garnet lherzolites have much higher Al_2O_3 (2.7-4.6 wt%) and lower olivine Fo (87.0-90.9) than those of spinel harzburgites (0.9-2.3 wt%; 90.6-92.3). Most samples scatter around the expected melting trend defined by the low-T peridotites (Fig. 3A). Two garnet lherzolites display clear deviations below this melting trend due to their low olivine Fo. The high-T spinel

harzburgites show degrees of melt-depletion similar to the low-T peridotites. The differences in spinel Cr# likely reflect differences in equilibration temperatures (Fig. 3B).

Despite the small data set (n=12), Re and Os concentrations and Os isotope compositions in the high-T peridotites vary considerably, although they are restricted to the ranges of oceanic peridotites and the low-T Malaita peridotites (Figs. 4 and 5). As expected from the incompatible behavior of Re and strongly compatible behavior of Os during mantle melting, spinel harzburgites (0.003-0.12 ppb) tend to have slightly lower Re than garnet lherzolites (0.02-0.58 ppb), while there is no discernible difference in their Os concentration ranges (1.6-4.6 ppb and 1.0-4.9 ppb, respectively).

The measured $^{187}\text{Os}/^{188}\text{Os}$ appear to display systematic variations reflecting the differences in rock type. Garnet lherzolites with slightly depleted characteristics (olivine Fo=90-91) show uniform $^{187}\text{Os}/^{188}\text{Os}$ ratios of 0.1244-0.1254, despite a wide range of $^{187}\text{Re}/^{188}\text{Os}$ ratios (0.05 to 0.82; Fig. 6). More depleted rocks such as spinel harzburgites, characterized by low $^{187}\text{Re}/^{188}\text{Os}$ (0.01-0.15), possess distinctively unradiogenic $^{187}\text{Os}/^{188}\text{Os}$ ratios of 0.1168-0.1196 which are distinguishable from most of the low-T harzburgites in terms of present-day $^{187}\text{Os}/^{188}\text{Os}$ ratios, despite both harzburgite groups recording similar degrees of melt-depletion (Fig. 3A). However, in terms of ingrowth-corrected $^{187}\text{Os}/^{188}\text{Os}$ ratios (assuming 122 Ma), a minor group of the low-T harzburgites is similar to the high-T harzburgites. Two Fe-enriched garnet lherzolites (SAG21 and SAG27) define the highest and lowest $^{187}\text{Os}/^{188}\text{Os}$ ratios of the high-T peridotites and hence there is no isotopic relationship with Fe-enrichment. Overall, the high-T peridotites are characterized by a bimodal distribution of $^{187}\text{Os}/^{188}\text{Os}$ ratios, whereas more radiogenic compositions dominate the low-T peridotites, although a minor unradiogenic peak is also evident (Figs. 5-7).

4. Discussion

4.1. Assessing secondary processes

Because we examined a mixture of fresh, unmetasomatised and altered, modally metasomatised samples, it is prudent to evaluate these influences on the Re-Os systematics before discussing potential mantle source information. For instance, the data scattering observed between the $^{187}\text{Os}/^{188}\text{Os}$ ratios and melt depletion indicators could be related to Re and/or Os mobility during syn- and post-eruptive alteration (e.g. host alnöite infiltration and surficial alteration) or mantle metasomatism (e.g. melt-rock reaction associated with or without modal changes) after initial melt depletion.

4.1.1. Syn- and post-eruptive alteration

Loss on ignition (LOI; wt%) is an indicator of the overall level of alteration because the degree of preservation of fresh olivine and orthopyroxene principally control LOI variations in peridotites. No covariation exists between LOI values (0-7 wt%) and Re-Os concentrations or $^{187}\text{Re}/^{188}\text{Os}$ - $^{187}\text{Os}/^{188}\text{Os}$ ratios among any rock types (Table 1, Fig. S1). This suggests that there is no systematic effect of surficial alteration on the xenolith Re-Os systematics. Similar conclusions have been derived from studies on abyssal peridotites, which have experienced greater degrees of serpentinisation and seafloor weathering, with significantly higher LOI (9-16 wt%; Harvey et al., 2006; Liu et al., 2008).

Another process that potentially might have affected the Malaita xenoliths is the breakdown of sulfide, the main host of Re and Os in typical peridotites (Burton et al., 1999; Alard et al., 2000). Several authors have suggested that sulfide breakdown is relatively common for peridotite xenoliths during rapid eruption of the host magma, probably through volatilization under oxygenated conditions (Handler et al., 1999), or during percolation of sulfur-undersaturated melt associated with host volcanism

(Reisberg et al., 2005). These processes have been invoked to explain the well-documented fact that the basalt-borne peridotite xenoliths from off-craton regions display systematic depletions of S, Re and Os (e.g. elevated Cu/S or Ir/Os ratios) relative to those in massif peridotite and kimberlite-derived cratonic xenoliths (e.g. Pearson et al., 2004; Rudnick and Walker, 2009). In the case of oceanic mantle (Fig. 4C), the mean Os concentration of peridotite xenoliths is slightly lower than that in abyssal peridotites, and this difference could result from sulfide breakdown processes. However, no such processes have been recognized thus far, even during detailed studies of sulfide petrography and highly siderophile element behavior (e.g. Lorand et al., 2004).

In the case of Malaitan peridotite xenoliths, the lack of significant Os loss is clearly indicated by a very pronounced mode in Os concentrations close to the PUM value (Fig. 4D). Although there is a secondary mode in Os concentrations at less than 1 ppb, this is essentially comprised of the low-T harzburgite group, and it seems unlikely that secondary alteration preferentially disturbed the harzburgites. Moreover, the low-T harzburgites yield correlations between $^{187}\text{Re}/^{188}\text{Os}$ and $^{187}\text{Os}/^{188}\text{Os}$ ratios, which can be interpreted as having age significance (Fig. 6A inset). Note that neither array is a mixing trend caused by infiltration of seawater or the host alnöite; seawater and alnöite are characterized by $^{187}\text{Re}/^{188}\text{Os}$ and $^{187}\text{Os}/^{188}\text{Os}$ values that plot well below and above these arrays, respectively (seawater, $^{187}\text{Re}/^{188}\text{Os} \sim 4000$, $^{187}\text{Os}/^{188}\text{Os} \sim 1$; alnöite $^{187}\text{Re}/^{188}\text{Os} \sim 0.25$, $^{187}\text{Os}/^{188}\text{Os} \sim 0.155$). Thus, syn- and post-eruptive alteration processes do not offer a reasonable explanation for the Re-Os variation observed in the Malaitan xenoliths. This, in turn suggests that the overall variation was likely created by processes occurring before the xenolith emplacement.

4.1.2. Mantle metasomatism

Within the Malaita peridotite suite, there are a number of indications of

overprinting by reaction with percolating melts or fluids. For example, some samples contain texturally equilibrated amphibole (limited to low-T peridotite groups), low-Fo olivine and clinopyroxene with elevated incompatible elements such as Na and Ti contents (Neal, 1988; Ishikawa et al., 2004). If such metasomatic processes had a significant impact on the Re-Os systematics, we may expect a correlation of $^{187}\text{Os}/^{188}\text{Os}$ with degree of metasomatism. No systematic variation exists. For example, amphibole-rich (>10 vol%) lherzolites and harzburgites (SAS45, SAG22, SAG6, SAS27, SAS56) possess subchondritic $^{187}\text{Os}/^{188}\text{Os}$ ratios, which are indistinguishable from other less metasomatised samples. Sample SAG3 has elevated (supra-PUM) Al and Re contents and also the highest $^{187}\text{Os}/^{188}\text{Os}$ ratio of the suite. However, this sample has an overabundance of garnet and does not contain a significant amount of modal amphibole. Hence, processes other than amphibole introduction are likely to control the anomalous composition of this sample, such enrichment in Al_2O_3 and Re from melt infiltration, with the highly radiogenic $^{187}\text{Os}/^{188}\text{Os}$ ratio reflecting radiogenic in-growth.

Other geochemical data provide further evidence that Os isotopic compositions have not been significantly changed by the recent metasomatism. The spinel lherzolites with the highest and lowest $^{187}\text{Os}/^{188}\text{Os}$ ratios (SAS32 and SAS41, respectively) were both assigned to the least-metasomatised group based on trace element and Sr-Nd isotopic compositions of constituent clinopyroxene (Ishikawa et al., 2005). The sample SAS32 preserves an unradiogenic Sr composition of 0.7029 and, together with the other least metasomatised peridotites, a Sm-Nd isotopic record of melt depletion at c.a. 160 Ma. The anomalously low $^{187}\text{Os}/^{188}\text{Os}$ ratio found in sample SAS41 complements its anomalously high initial ϵ_{Nd} value of +16.4 recorded in clinopyroxene. Thus, it is likely that Os isotope variations are primarily controlled by pre-existing heterogeneity in the source peridotite.

High-T peridotites do not contain volatile-bearing phases such as amphibole, but there is evidence of metasomatic enrichment caused by percolating melt in the

compositions of their constituent minerals (Ishikawa et al., 2004). In particular, garnet
 lherzolites SAG21 and SAG27, derived from the deepest portion of the lithosphere (3.3
 and 3.4 GPa, respectively), contain minerals with low Mg-numbers (e.g. low-Fo
 olivine) which give rise to clear deviations below the overall melting trend in the Al_2O_3
 vs. Fo diagram (Fig 3B). Retention of core-rim zonation in garnets suggests that
 Fe-enrichment of these samples probably occurred recently (Ishikawa et al., 2004). This
 Fe-metasomatism can be attributed, on the basis of mineral chemistry, to melt-mediated
 chemical interaction with pyroxenites, which occur in Malaita as a suite of xenoliths
 derived from the same depth interval. As $^{187}\text{Os}/^{188}\text{Os}$ ratios of the garnet
 clinopyroxenites vary greatly from 0.17 to 5 (Ishikawa et al., 2009), we would expect
 that $^{187}\text{Os}/^{188}\text{Os}$ ratios in metasomatised peridotites may be elevated, if the Re-Os
 system has been significantly perturbed. In contrast, all high-T peridotites including the
 Fe-enriched garnet lherzolites have unradiogenic $^{187}\text{Os}/^{188}\text{Os}$, suggesting that the effect
 of pyroxenite interaction on $^{187}\text{Os}/^{188}\text{Os}$ ratios has been minimal, possibly due to the
 combined effects of the low Os concentrations in pyroxenite-derived melts and the
 recent nature of the chemical interaction. Indeed, the similarity of $^{187}\text{Os}/^{188}\text{Os}$ ratios
 between SAG27 and spinel harzburgites, suggests that refertilization of former
 harzburgite may be responsible for the present fertile major element chemical
 composition of SAG27, while the sample retains the Os isotope memory of the
 precursor.

In summary, the wide range of $^{187}\text{Os}/^{188}\text{Os}$ compositions observed in Malaita
 peridotites are not systematically affected by disturbance due to secondary processes
 such as recent low-T alteration or metasomatism, but instead mostly reflect long-term
 heterogeneity in the source peridotite which provides useful chronological information.
 This is in agreement with the conclusion of the other Re-Os isotope studies of oceanic
 mantle (e.g. Liu et al., 2008).

4.2. *Re-Os Ages*

4.2.1 *Mechanism and timing of low-T harzburgite formation*

The two linear arrays defined by the low-T harzburgites in the Re-Os isochron diagram (Fig. 6 inset) yield apparent ages of 111 ± 24 and 129 ± 10 Ma for main and unradiogenic groups, respectively. Although they are not isochrons, these apparent ages are within uncertainty of the 126-119 Ma range of the Ontong Java Plateau magmatism determined by Ar-Ar and Re-Os dating of plateau basalts (Mahoney et al., 1993; Tejada et al., 1996; Parkinson et al., 2002; Tejada et al., 2002). This coincidence supports their chronological significance, and moreover implies a genetic relationship between plateau basalts and the low-T harzburgites. Since the variation in $^{187}\text{Re}/^{188}\text{Os}$ in the low-T harzburgites is largely controlled by variable degree of Os depletion, the inferred age appears to represent the timing of Os removal. The fact that only the low-T harzburgite group contains low Os samples (<1 ppb) could be used to suggest that the transformation to harzburgite is responsible for lowering Os content. The strongly compatible behavior of Os during mantle melting argues against this hypothesis; melt depletion normally leads to higher Os contents in refractory harzburgites than precursor peridotites in cratonic and massif peridotites (e.g. Pearson et al., 2004). An alternative model is that the formation of the Malaita low-T harzburgites results from melt-peridotite reaction involving dissolution of garnet and pyroxenes and precipitation of new forsteritic olivine (e.g., Kelemen et al., 1992). The infiltration of sulfur-undersaturated basaltic or picritic melts at high melt/rock ratio can lead to dissolution of sulfide together with garnet and pyroxenes from host peridotites. Since Os is located almost exclusively in sulfide, while a significant fraction of Re could reside in silicate (Burton et al., 2000; Luguet et al., 2007), the resulting harzburgites are expected to have elevated Re/Os ratios, as observed in some of the low-T harzburgites. The systematic decrease in Os content and resulting increase of Re/Os due to

progressive melt-peridotite reaction has been well documented in a dunite channel from the Troodos ophiolite (Büchl et al., 2002). Moreover, similar processes have been implicated in the formation of bimodal suites of fertile lherzolites and refractory harzburgites derived from different depth intervals along the northern Canadian Cordillera (Peslier et al., 2000).

A model of harzburgite formation by remelting of a dominantly lherzolitic lithosphere triggered by the percolation of melts or fluid into the lithospheric base, such as proposed by Peslier et al. (2000), could be applicable to the generation of the Malaita low-T harzburgites. Equilibrium temperatures place the majority of the low-Os harzburgites below the lherzolite-dominated upper lithosphere (Fig. 8A), suggesting that the low-T lherzolites and the harzburgites do not share a common origin through simple melt extraction due to adiabatic decompression (Ishikawa et al., 2004). This is also supported by ages of ca. 111-130 Ma defined on Re-Os isochron correlation diagrams by the harzburgites (Fig. 6). These ages are younger than the Sm-Nd isochron age of ca. 160 Ma for lithosphere formation in a mid-oceanic ridge setting (Ishikawa et al., 2005). Thus, a likely scenario is that the harzburgites were formed through open-system melting of a ~160 Ma lower lithosphere induced by infiltration of sulfur-undersaturated magma related to ca. 122 Ma Ontong Java Plateau activity. This scenario is consistent with the sulfur-undersaturated nature of the erupted plateau basalts (Chazey and Neal, 2004; Roberge et al., 2004), whose primary magma is thought to coexist with harzburgite at moderate high-pressure conditions (2-3 GPa; Herzberg, 2004).

A difficulty with the above model is that the plateau basalts display PUM-like initial $^{187}\text{Os}/^{188}\text{Os}$ ratios (0.1295 ± 11 ; Parkinson et al., 2002), in contrast to the unradiogenic $^{187}\text{Os}/^{188}\text{Os}$ initial ratios (main group: 0.1236 ± 6 ; unradiogenic group: 0.1163 ± 5) of the low-T harzburgites. However, the melt percolation process can occur without the attainment of Os isotopic equilibrium because the principal reaction controlling the Re-Os systematics is the dissolution of sulfide exposed to the migrating

melt. Osmium isotopic disequilibrium between interstitial sulfides and sulfide inclusions trapped in silicates has been frequently observed in natural peridotites, and has been commonly interpreted as a consequence of melt percolation (Burton et al., 1999; Alard et al., 2002). We therefore envisage that there was no subsequent sulfide precipitation from the melt and the remaining Os in the low-T harzburgites is principally hosted in minor sulfide inclusions shielded from intergranular melt. This can account for the difference in Os isotope composition of infiltrated magma (related to Ontong Java Plateau basalts) and their reaction products. The above scenario is also attractive in terms of explaining why the two groups of harzburgites cannot be differentiated based on petrography and chemistry. They have acquired their depleted character during percolation of almost identical melts, which results in significant loss of Os without modification of original $^{187}\text{Os}/^{188}\text{Os}$ ratios.

An alternative scenario is that the low-T harzburgites were originally formed as residues after melt extraction and then underwent Os loss associated with late-stage metasomatism. This scenario may be attractive if we consider that the low-T harzburgites represent the upper-layer of upwelling mantle accreted to the base of pre-existing lherzolitic lithosphere. However, at the present state of our knowledge, it seems difficult to explain why the metasomatism responsible for Os removal is only operative preferentially for the low-T harzburgites. Thus, a detailed mechanism for the formation of the low-T harzburgites deserves further study and would offer further insights into the relationships between the plateau basalts and underlying lithosphere.

4.2.2 Model ages – timing of melt depletion

Despite the lack of isochronous behavior for the majority of Malaita peridotites, the timing of melt depletion can be estimated for individual samples using the model age concept. Any recent disturbance of the Re-Os system renders model ages calculated using measured $^{187}\text{Re}/^{188}\text{Os}$ ratios unreliable. This is particularly true for Malaita

peridotites which have probably been extensively affected by 122 Ma Ontong Java Plateau magmatism (e.g. low-T harzburgites which display large Re/Os variations). As an alternative we employ the Re-depletion model age (T_{RD}) to translate peridotite Os isotope data into minimum ages of depletion, assuming that a single melting event quantitatively removed Re (Walker et al., 1989). We calculate T_{RD} ages at 122 Ma ($T_{RD-122\text{ Ma}}$) assuming that measured Re/Os ratios have persisted since the time of Ontong Java Plateau magmatism. Such $T_{RD-122\text{ Ma}}$ ages will always yield ages slightly older than the simple T_{RD} ages as the latter assume no ingrowth of ^{187}Os since plateau formation.

Another source of model age uncertainty relates to the selection of the model reservoir. PUM reservoirs may not be appropriate, particularly for dating young, Phanerozoic peridotites because it is unrealistic to assume recent convective mantle is dominated by such primitive material (e.g. Rudnick and Walker, 2009). Instead, we use two different mantle evolution models for calculating T_{RD} and $T_{RD-122\text{ Ma}}$ ages: T_{RD} ages were calculated using the overall chondrite average ($^{187}\text{Os}/^{188}\text{Os}=0.1276$, $^{187}\text{Re}/^{188}\text{Os}=0.397$; Walker et al., 2002); whereas $T_{RD-122\text{ Ma}}$ ages are calculated using a combined data set for two Os-rich platinum-group alloy (PGA) suites derived from recently emplaced ophiolites (southwestern Oregon and northern California, 165 Ma; Tibet, 95 Ma), which yields an average $^{187}\text{Os}/^{188}\text{Os}$ ratio of 0.1251 for a depleted mantle source ($n=1116$; Meibom and Frei, 2002; Meibom et al., 2002; Walker et al., 2005; Pearson et al., 2007; Shi et al., 2007; Luguet et al., 2008). This equates to an unradiogenic present-day $^{187}\text{Os}/^{188}\text{Os}$ ratio of 0.1259 (assuming chondritic evolution since 122 Ma). Thus, most $T_{RD-122\text{ Ma}}$ ages are significantly younger than simple T_{RD} ages calculated assuming chondritic mantle evolution (Table 1).

On the basis of T_{RD} ages, there are two populations of the $^{187}\text{Os}/^{188}\text{Os}$ ratios in the Malaita peridotites. The main population (55 of 70 samples) yields T_{RD} ages of -0.2 to 0.8 Ga (Table 1, Fig 5). A subordinate population (11 of 70 samples) gives

Proterozoic model T_{RD} ages of 1.1 to 1.8 Ga. Using $T_{RD-122\text{ Ma}}$ ages (Fig. 7), the main population is recast as -0.4 to 0.7 Ga and the unradiogenic population gives ages of 0.9 to 1.7 Ga. The average difference in T_{RD} and $T_{RD-122\text{ Ma}}$ ages is about ~170 Ma (average values of the main population T_{RD} ~290 Ma and $T_{RD-122\text{ Ma}}$ ~120 Ma) and principally reflects the choice of reference reservoir. The $T_{RD-122\text{ Ma}}$ ages of the main population provide plausible estimates for normal Jurassic-Cretaceous mantle. The older ages clearly represent ancient mantle that experienced high degree melt extraction in the Meso-Proterozoic, emplaced beneath the Ontong Java Plateau. These ancient samples are far more common in high-T (deep) peridotite suite (Fig. 7), indicating uneven depth-distribution of the ancient mantle within the subplateau lithosphere.

4.3. Origin of ancient osmium signatures

There are several potential explanations for the diversity of ancient Os signatures found in the oceanic lithosphere underlying the Ontong Java Plateau. Ancient depleted subcontinental mantle is characterized by very unradiogenic Os whose ancient model ages (e.g. Walker et al., 1989; Carlson et al., 2005; Pearson and Wittig, 2008) reflect their isolation from the convecting mantle for billions of years. Such material could underlie the Ontong Java Plateau. An analogous scenario was suggested for mantle beneath the Kerguelen Plateau to account for unradiogenic Os isotope compositions (≥ 0.1189) found in some Kerguelen harzburgite xenoliths (Hassler and Shimizu, 1998). However, unlike the Kerguelen Plateau where several lines of evidence support the involvement of continental fragments (see Frey et al., 2002), the consensus of previous work on the Ontong Java Plateau indicates its generation in an essentially oceanic setting, within the Pacific Plate, far removed from any known continental boundaries (e.g. Kroenke et al., 2004). Hence the involvement of ancient continental lithosphere seems unlikely. Tectonic underplating of old subcontinental mantle can also be ruled out because plate reconstructions indicate that xenolith entrainment occurred in

an intraplate setting within the subducting Pacific plate, well before the initiation of collision-related deformation of the plateau against the overlying Australia Plate (Fig. 1).

Another hypothesis is that the Ontong Java Plateau lithosphere may reflect the inherent isotopic variability of the oceanic mantle as represented by abyssal peridotites, within which our data largely fall (Fig. 5). Although the majority of abyssal peridotites possess $^{187}\text{Os}/^{188}\text{Os}$ in the range from 0.120 to 0.130, recent studies of the Mid-Atlantic ridge and the ultra-slow spreading Gakkel ridge demonstrate the presence of samples with much lower $^{187}\text{Os}/^{188}\text{Os}$, extending as low as 0.1139 (Harvey et al., 2006; Liu et al., 2008). Furthermore, sulfide grains recovered from abyssal peridotites show significant Os isotopic heterogeneity between individual grains within a single sample (Alard et al., 2005; Harvey et al., 2006). This evidence, along with the even larger isotopic diversity of PGAs derived from ophiolites (e.g. Meibom et al., 2002; Pearson et al., 2007) has led many researchers to postulate that the oceanic upper mantle retains Os isotopic signatures of ancient melting events, which are resistant to subsequent convective mixing. Within this context, it is possible to interpret the Os isotopic diversity observed in Malaita peridotites as merely representing the unmixed heterogeneity in the convective upper mantle. However, the sharp contrast between the Os isotopic distributions of shallow and deep Malaita peridotites (Fig. 7) is difficult to explain by mantle heterogeneity alone. The low-T peridotites show remarkable correspondence to the combined data set for PGAs from the Jurassic-Cretaceous ophiolites, supporting their derivation from the same mantle reservoir. In contrast, the bimodal distribution of the high-T peridotites is distinctive and unradiogenic $^{187}\text{Os}/^{188}\text{Os}$ ratios less than 0.120 are statistically abundant. This suggests that the deep lithosphere is sampling a different mantle reservoir from the normal shallow convective upper mantle represented by the low-T Malaita peridotites, PGA grains and the majority of abyssal peridotites.

A model that can explain the relationship between depth and isotopic

heterogeneity in the Malaita peridotites involves the deepest plateau lithosphere as representing recycled heterogeneity within the upwelling mantle source of Ontong Java Plateau magmatism. A similar model has recently been suggested for Salt Lake Crater peridotite xenoliths from Hawaii (Bizimis et al., 2007), which, strikingly, have an almost identical statistical distribution of Os isotope compositions to the high-T Malaita peridotites (Fig. 7). In the case of the Ontong Java Plateau lithosphere, peridotites with ancient depletion ages are strongly focused in the lower section of the lithosphere (>95 km) lying under pre-existing 160 Ma Pacific lithosphere comprised of the low-T lherzolites and just beneath a layer of low-Os harzburgites (Fig. 8). Hence, we suggest that the basal section of subplateau lithosphere represents the residual mantle left behind after Ontong Java magmatism, incorporating significant amounts of ancient recycled components.

In Fig. 8, we attempt to illustrate that the Os isotopic compositions of Malaita peridotites are consistent with the lithosphere underlying the Ontong Java Plateau consisting of shallower oceanic lithosphere and deeper impinged material. The involvement of ancient recycled components in this ascending material has previously been identified by the existence of recycled garnet pyroxenites of Proterozoic age (0.5-1 Ga) in the basal section of the subplateau lithosphere (Nd-Hf-Pb; Ishikawa et al., 2007). Broadly comparable ages obtained from the high-T harzburgites (T_{RD-122} Ma age mode ~1.1 Ga) imply that the pyroxenites and deep peridotites could be regarded as fragments of the same crust-mantle section, introduced into the convecting mantle in the Proterozoic and subsequently incorporated into upwelling mantle that created the Ontong Java Plateau in the Cretaceous Pacific.

Implications for the Ontong Java Plateau

Malaita xenolith data indicate the presence of substantial heterogeneity in the upwelling mantle beneath the plateau, as represented by three different lithologies:

depleted harzburgite created by ancient melting, recycled eclogite/pyroxenite originating from ancient crust (Ishikawa et al., 2007) and fertile lherzolite typical of the convective mantle. Although a homogeneous peridotitic PUM-like source has been proposed for the Ontong Java Plateau basalts (Parkinson et al., 2002), the near total absence of the PUM-like $^{187}\text{Os}/^{188}\text{Os}$ ratios from the Malaita peridotite suite suggests that mixing and homogenization of composite magmas derived from radiogenic pyroxenites and unradiogenic peridotites may be responsible for the relatively uniform PUM-like lava compositions.

Whether the plateau was formed through upwelling of heterogeneous source mantle is relevant to the minor initial uplift of the plateau (Fig. 8D). However, unknown factors such as the relative abundances of the three lithologies and the relevant potential mantle temperature (T_p) preclude being able to place quantitative dynamical constraints of the chemical and physical characteristics of the upwelling mantle as a whole.

A relatively high fraction of dense eclogite/pyroxenite components would give voluminous melt at low- T_p , due to the higher melt productivity of eclogite/pyroxenite, obviating the need for very high- T_p mantle and reducing initial uplift (Fitton and Godard, 2004; Korenaga, 2005). However, it is doubtful that such low- T magma could lead to remelting of pre-existing lherzolitic lithosphere as indicated by the Cretaceous formation of a refractory harzburgite-layer ($\text{Fo}\sim 92$) now present at $\sim 85\text{--}90$ km depth (Fig. 8). Thus, we speculate that a hotter-than-ambient mantle must have played a role in the formation of the Ontong Java Plateau. However, the requirement of exceptionally high- T_p mantle ($>1600^\circ\text{C}$; Fig. 2) to account for the occurrence of deep harzburgite (>95 km) is circumvented because the harzburgites acquired their depleted character during the Proterozoic.

The residual mantle after plateau volcanism may have been rheologically strong, presumably due to chemical modification and/or complete dehydration associated with melting, allowing the residue to form a rigid basal section to the oceanic lithosphere.

Such mechanical coupling is required because the fragments of the residue, generated at 122 Ma, were brought to the surface as xenoliths 90 Ma later, when the plateau had migrated away from its generation site. This suggests that the Ontong Java Plateau lithosphere thickened abruptly at the time of plateau generation, implying that the evolution of this accreted residue played an essential role in the subsidence history of the plateau. Surface wave tomography has revealed the presence of a low-velocity root reaching to a depth of 300 km beneath the central high plateau (Richardson et al., 2000; Klosko et al., 2001; Gomer and Okal, 2003). This has been interpreted as the residual mantle root of the Ontong Java Plateau magmatism, with a chemically anomalous nature. Such an observation is apparently consistent with the xenolith studies, although Malaita xenoliths may only represent the peripheral thinner lithosphere (~120 km). Thus, higher resolution tomography to constrain internal and external structures of this root will be critical to obtaining a more complete picture of the subplateau lithosphere and may provide new insights into the nature and origin of the Ontong Java Plateau.

Acknowledgments

We are grateful to Shigenori Maruyama, Tsuyoshi Komiya and the Solomon Islands Geological Survey for field assistance and to Geoff Nowell, Chris Ottley and Nick Marsh for analytical support. Constructive reviews by two anonymous referees are greatly appreciated. This study was supported by JSPS Postdoctoral Fellowships for Research Abroad to AI.

References

- Alard, O., Griffin, W.L., Lorand, J.-P., Jackson, S.E., O'Reilly, S.Y., 2000. Non-chondritic distribution of the highly siderophile elements in mantle sulphides. *Nature* 407, 891-894.
- Alard, O., Griffin, W.L., Pearson, N.J., Lorand, J.-P., O'Reilly, S.Y., 2002. New insights into the Re-Os systematics of sub-continental lithospheric mantle from in situ analysis of sulphides. *Earth Planet. Sci. Lett.* 203, 651-663.
- Alard, O., Luguet, A., Pearson, N.J., Griffin, W.L., Lorand, J.-P., Gannoun, A., Burton, K.W., O'Reilly, S.Y., 2005. In-situ Os isotopes in abyssal peridotites bridge the isotopic gap between MORBs and their source mantle. *Nature* 436, 1005-1008.
- Becker, H., Horan, M.F., Walker, R.J., Gao, S., Lorand, J.-P., Rudnick, R.L., 2006. Highly siderophile element composition of the Earth's primitive upper mantle: Constraints from new data on peridotite massifs and xenoliths. *Geochim. Cosmochim. Acta* 70, 4528-4550.
- Bizimis, M., Griselein, M., Lassiter, J.C., Salters, V.J.M., Sen, G., 2007. Ancient recycled mantle lithosphere in the Hawaiian plume: Osmium-Hafnium isotopic evidence from peridotite mantle xenoliths. *Earth Planet. Sci. Lett.* 257, 259-273.
- Brey, G.P., Köhler, T., 1990. Geothermobarometry in four-phase lherzolites II. New thermobarometers, and practical assessment of existing thermobarometers. *J. Petrol.* 31, 1352-1378.
- Büchl, A., Brüggmann, G.E., Batanova, V.G., Münker, C., Hofmann, A.W., 2002. Melt percolation monitored by Os isotopes and HSE abundances: a case study from the mantle section of the Troodos ophiolite. *Earth Planet. Sci. Lett.* 204, 385-402.
- Burton, K.W., Schiano, P., Birck, J.-L., Allègre, C.J., 1999. Osmium isotope disequilibrium between mantle minerals in a spinel-lherzolite. *Earth Planet. Sci. Lett.* 172, 311-322.
- Burton, K.W., Schiano, P., Birck, J.-L., Allègre, C.J., Rehkämper, M., Halliday, A.N., Dawson, J.B., 2000. The distribution and behaviour of rhenium and osmium amongst mantle minerals and the age of the lithospheric mantle beneath Tanzania. *Earth Planet. Sci. Lett.* 183, 93-106.
- Carlson, R.W., Pearson, D.G., James, D.E., 2005. Physical, chemical, and chronological characteristics of continental mantle. *Rev. Geophys.* 43, 1-24.
- Chazey, W.J., III., Neal, C.R., 2004. Large igneous province magma petrogenesis from source to surface: platinum-group element evidence from Ontong Java Plateau basalts recovered during ODP Leg 130 and 192. In: Fitton, J.G., Mahoney, J.J., Wallace, P.J., Saunders, A.D. (Eds.), *Origin and Evolution of the Ontong Java Plateau*. Geological Society of London, London, pp. 219-238.
- Courtillot, V., Olson, P., 2007. Mantle plumes link magnetic superchrons to Phanerozoic mass depletion events. *Earth Planet. Sci. Lett.* 260, 495-504.
- Dale, C.W., Pearson, D.G., Starkey, N.A., Stuart, F.M., Ellam, R.M., Larsen, L.M., Fitton, J.G., Macpherson, C.G., 2009. Osmium isotopes in Baffin Island and West Greenland picrites: implications for the $^{187}\text{Os}/^{188}\text{Os}$ composition of the convecting

645 mantle and the nature of high $^3\text{He}/^4\text{He}$ mantle. *Earth Planet. Sci. Lett.* 278, 266-277.

646 Fitton, J.G., Godard, M., 2004. Origin and evolution of magmas on the Ontong Java
647 Plateau. In: Fitton, J.G., Mahoney, J.J., Wallace, P.J., Saunders, A.D. (Eds.), *Origin*
648 *and Evolution of the Ontong Java Plateau*. Geological Society of London, London,
649 pp. 151-178.

650 Frey, F.A., Weis, D., Borisova, A.Y., Xu, G., 2002. Involvement of continental crust in
651 the formation of the Cretaceous Kerguelen Plateau: new perspective from ODP Leg
652 120 sites. *J. Petrol.* 43, 1207-1239.

653 Gomer, B.M., Okal, E.A., 2003. Multiple-ScS probing of the Ontong-Java Plateau. *Phys.*
654 *Earth Planet. Inter.* 138, 317-331.

655 Hall, R., 2002. Cenozoic geological and plate tectonic evolution of SE Asia and the SW
656 Pacific: computer-based reconstructions, model and animations. *J. Asian Earth Sci.*
657 20, 353-431.

658 Handler, M.R., Bennett, V.C., Dreibus, G., 1999. Evidence from correlated Ir/Os and
659 Cu/S for late-stage Os mobility in peridotite xenoliths: implications for Re-Os
660 systematics. *Geology* 27, 75-78.

661 Harvey, J., Gannoun, A., Burton, K.W., Rogers, N.W., Alard, O., Parkinson, I.J., 2006.
662 Ancient melt extraction from the oceanic upper mantle revealed by Re-Os isotopes
663 in abyssal peridotites from the Mid-Atlantic ridge. *Earth Planet. Sci. Lett.* 244,
664 606-621.

665 Hassler, D.R., Shimizu, N., 1998. Osmium isotopic evidence for ancient subcontinental
666 lithospheric mantle beneath the Kerguelen Islands, Southern Indian Ocean. *Science*
667 280, 418-441.

668 Hauri, E.H., 1992. Geochemical and fluid dynamic investigations into the nature of
669 chemical heterogeneity in the Earth's mantle, MIT & Woods Hole Oceanographic
670 Institution, 239 pp.

671 Herzberg, C.T., 2004. Geodynamic information in peridotite petrology. *J. Petrol.* 45,
672 2507-2530.

673 Herzberg, C.T., 2004. Partial melting below the Ontong Java Plateau. In: Fitton, J.G.,
674 Mahoney, J.J., Wallace, P.J., Saunders, A.D. (Eds.), *Origin and Evolution of the*
675 *Ontong Java Plateau*. Geological Society of London, London, pp. 179-183.

676 Ingle, S., Coffin, M.F., 2004. Impact origin for the greater Ontong Java Plateau? *Earth*
677 *Planet. Sci. Lett.* 218, 123-134.

678 Ishikawa, A., Maruyama, S., Komiya, T., 2004. Layered lithospheric mantle beneath the
679 Ontong Java Plateau: implications from xenoliths in alnöite, Malaita, Solomon
680 Islands. *J. Petrol.* 45, 2011-2044.

681 Ishikawa, A., Nakamura, E., Mahoney, J.J., 2005. Jurassic oceanic lithosphere beneath
682 the southern Ontong Java Plateau: evidence from xenoliths in alnöite, Malaita,
683 Solomon Islands. *Geology* 33, 393-396.

684 Ishikawa, A., Pearson, D.G., Dale, C.W., 2009. Re-Os isotopes and platinum-group
685 elements in a peridotite-pyroxenite hybrid mantle. *Geochim. Cosmochim. Acta* 73,
686 A572-A572.

- 687 Ishikawa, A., Kuritani, T., Makishima, A., Nakamura, E., 2007. Ancient recycled crust
688 beneath the Ontong Java Plateau: isotopic evidence from the garnet clinopyroxenite
689 xenoliths, Malaita, Solomon Islands. *Earth Planet. Sci. Lett.* 259, 134-148.
- 690 Kelemen, P.B., Dick, H.J.B., Quick, J.E., 1992. Formation of harzburgite by pervasive
691 melt/rock interaction in the upper mantle. *Nature* 358, 635-641.
- 692 Kerr, A.C., Mahoney, J.J., 2007. Oceanic plateaus: problematic plumes, potential
693 paradigms. *Chem. Geol.* 241, 332-353.
- 694 Klosko, E.R., Russo, R.M., Okal, E.A., Richardson, W.P., 2001. Evidence for a
695 rheologically strong chemical mantle root beneath the Ontong-Java Plateau. *Earth*
696 *Planet. Sci. Lett.* 186, 347-361.
- 697 Korenaga, J., 2005. Why did not the Ontong Java Plateau form subaerially? *Earth Planet.*
698 *Sci. Lett.* 234, 385-399.
- 699 Kroenke, L.W., Wessel, P., Sterling, A., 2004. Motion of the Ontong Java Plateau in the
700 hotspot frame of reference: 122 Ma-present. In: Fitton, J.G., Mahoney, J.J., Wallace,
701 P.J., Saunders, A.D. (Eds.), *Origin and Evolution of the Ontong Java Plateau.*
702 *Geological Society of London, London*, pp. 9-20.
- 703 Liu, C.-Z., Snow, J.E., Hellebrand, E., Brüggmann, G., Von der Handt, A., Büchl, A.,
704 Hofmann, A.W., 2008. Ancient, highly heterogeneous mantle beneath Gakkel ridge,
705 Arctic Ocean. *Nature* 452, 311-316.
- 706 Lorand, J.-P., Delpech, G., Gregoire, M., Moine, B., O'Reilly, S.Y., Cottin, J.-Y., 2004.
707 Platinum-group elements and the multistage metasomatic history of Kerguelen
708 lithospheric mantle (South Indian Ocean) *Chem. Geol.* 208, 195-215.
- 709 Luguet, A., Nowell, G.M., Pearson, D.G., 2008. $^{184}\text{Os}/^{188}\text{Os}$ and $^{186}\text{Os}/^{188}\text{Os}$
710 measurements by Negative Thermal Ionisation Mass Spectrometry (N-TIMS):
711 effects of interfering element and mass fractionation corrections on data accuracy
712 and precision. *Chem. Geol.* 248, 342-362.
- 713 Luguet, A., Shirey, S.B., Lorand, J.-P., Horan, M.F., Carlson, R.W., 2007. Residual
714 platinum-group minerals from highly depleted harzburgites of the Lherz massif
715 (France) and their role in HSE fractionation of the mantle. *Geochim. Cosmochim.*
716 *Acta* 71, 3082-3097.
- 717 Luguet, A., Pearson, D.G., Nowell, G.M., Dreher, S.T., Coggon, J.A., Spetsius, Z.V.,
718 Parman, S.W., 2008. Enriched Pt-Re-Os isotope systematics in plume lavas
719 explained by metasomatic sulfides. *Science* 319, 453-456.
- 720 Mahoney, J.J., Storey, M., Duncan, R.A., Spencer, K.J., Pringle, M., 1993.
721 Geochemistry and geochronology of Leg 130 basement lavas: nature and origin of
722 the Ontong Java Plateau. *Proc. ODP, Sci. Results* 130, 3-22.
- 723 McDonough, W.F., Sun, S.-S., 1995. The composition of the Earth. *Chem. Geol.* 120,
724 223-253.
- 725 Meibom, A., Frei, R., 2002. Evidence for an ancient osmium isotopic reservoir in Earth.
726 *Science* 296, 516-518.
- 727 Meibom, A., Sleep, N.H., Chamberlain, C.P., Coleman, R.G., Frei, R., Hren, M.T.,
728 Wooden, J.L., 2002. Re-Os isotopic evidence for long-lived heterogeneity and
729 equilibration processes in the Earth's upper mantle. *Nature* 419, 705-708.

- 730 Meisel, T., Walker, R.J., Irving, A.J., Lorand, J.-P., 2001. Osmium isotopic compositions
731 of mantle xenoliths: a global perspective. *Geochim. Cosmochim. Acta* 65,
732 1311-1323.
- 733 Miura, S., Suyehiro, K., Shinohara, M., Takahashi, N., Araki, E., Taira, A., 2004.
734 Seismological structure and implications of collision between the Ontong Java
735 Plateau and Solomon Island Arc from ocean bottom seismometer-airgun data.
736 *Tectonophysics* 389, 191-220.
- 737 Neal, C.R., 1988. The origin and composition of metasomatic fluids and amphiboles
738 beneath Malaita, Solomon Islands. *J. Petrol.* 29, 149-179.
- 739 Nixon, P.H., Boyd, F.R., 1979. Garnet bearing lherzolites and discrete nodule suites
740 from the Malaita alnoite, Solomon Islands, S.W. Pacific, and their bearing on
741 oceanic mantle composition and geotherm. In: Boyd, F.R., Meyer, H.O.A. (Eds.),
742 The mantle sample: Inclusions in kimberlite and other volcanics. American
743 Geophysical Union, Washington D.C., pp. 400-423.
- 744 Nixon, P.H., Neal, C.R., 1987. Ontong Java Plateau: deep-seated xenoliths from thick
745 oceanic lithosphere. *Mantle Xenoliths*. John Wiley, New York, 335-345 pp.
- 746 Parkinson, I.J., Schaefer, B.F., Arculus, R.J., 2002. A lower mantle origin for the world's
747 biggest LIP? a high precision Os isotope isochron from Ontong Java Plateau basalts
748 drilled on ODP Leg 192. *Geochim. Cosmochim. Acta* 66, A580.
- 749 Parsons, B., Sclater, J.G., 1977. An analysis of the variation of ocean floor bathymetry
750 and heat flow with age. *J. Geophys. Res.* 82, 803-827.
- 751 Pearson, D.G., Wittig, N., 2008. Formation of Archaean continental lithosphere and its
752 diamonds: the root of the problem. *J. Geol. Soc. London* 165, 895-914.
- 753 Pearson, D.G., Parman, S.W., Nowell, G.M., 2007. A link between large mantle melting
754 events and continent growth seen in osmium isotopes. *Nature* 449, 202-205.
- 755 Pearson, D.G., Irvine, G.J., Ionov, D.A., Boyd, F.R., Dreibus, G.E., 2004. Re–Os
756 isotope systematics and platinum group element fractionation during mantle melt
757 extraction: a study of massif and xenolith peridotite suites. *Chem. Geol.* 208, 29-54.
- 758 Peslier, A.H., Reisberg, L., Ludden, J., Francis, D., 2000. Re-Os constraints on
759 harzburgite and lherzolite formation in the lithospheric mantle: a study of northern
760 Canadian Cordillera xenoliths. *Geochim. Cosmochim. Acta* 64, 3061-3071.
- 761 Petterson, M.G., Neal, C.R., Mahoney, J.J., Kroenke, L.W., Saunders, A.D., Babbs, T.L.,
762 Duncan, R.A., Tolia, D., McGrail, B., 1997. Structure and deformation of north and
763 central Malaita, Solomon Islands: tectonic implications for the Ontong Java
764 Plateau-Solomon arc collision, and for the fate of oceanic plateaus. *Tectonophysics*
765 283, 1-33.
- 766 Puchtel, I.S., Walker, R.J., James, O.B., Kring, D.A., 2008. Osmium isotope and highly
767 siderophile element systematics of lunar impact melt breccias: implications for the
768 late accretion history of the Moon and Earth. *Geochim. Cosmochim. Acta* 72,
769 3022-3042.
- 770 Reisberg, L., Zhi, X.C., Lorand, J.-P., Wagner, C., Peng, Z.C., Zimmermann, C., 2005.
771 Re-Os and S systematics of spinel peridotite xenoliths from east central China:
772 evidence for contrasting effects of melt percolation. *Earth Planet. Sci. Lett.* 239,

- 773 286-308.
- 774 Richardson, W.P., Okal, E.A., Van del Lee, S., 2000. Rayleigh-wave tomography of the
775 Ontong Java Plateau. *Phys. Earth Planet. Inter.* 118, 29-51.
- 776 Roberge, J., White, R.V., Wallace, P.J., 2004. Volatiles in submarine basaltic glasses
777 from the Ontong Java Plateau (ODP Leg 192): implications for magmatic processes
778 and source region. In: Fitton, J.G., Mahoney, J.J., Wallace, P.J., Saunders, A.D.
779 (Eds.), *Origin and Evolution of the Ontong Java Plateau*. Geological Society of
780 London, London, pp. 239-257.
- 781 Roberge, J., Wallace, P.J., White, R.V., Coffin, M.F., 2005. Anomalous uplift and
782 subsidence of the Ontong Java Plateau inferred from CO₂ contents of submarine
783 basaltic glasses. *Geology* 33, 501-504.
- 784 Rudnick, R.L., Walker, R.J., 2009. Interpreting ages from Re–Os isotopes in peridotites.
785 *Lithos* 112S, 1083–1095.
- 786 Shi, R.D., Alard, O., Zhi, X.C., O'Reilly, S.Y., Pearson, N.J., Griffin, W.L., Zhang, M.,
787 Chen, X.M., 2007. Multiple events in the Neo-Tethyan oceanic upper mantle:
788 evidence from Ru–Os–Ir alloys in the Luobusa and Dongqiao ophiolitic podiform
789 chromitites, Tibet. *Earth Planet. Sci. Lett.* 261, 33-48.
- 790 Simon, N.S.C., Neumann, E.-R., Bonadiman, C., Coltorti, M., Delpech, G., Grégoire,
791 M., Widom, E., 2008. Ultra-refractory domains in the oceanic mantle lithosphere
792 sampled as mantle xenoliths at ocean islands. *J. Petrol.* 49, 1223-1251.
- 793 Stein, C.A., Stein, S., 1992. A model for the global variation in oceanic depth and
794 heat-flow with lithosphere age. *Nature* 359, 123-129.
- 795 Tejada, M.L.G., Mahoney, J.J., Duncan, R.A., Hawkins, M.P., 1996. Age and
796 geochemistry of basement and alkalic rocks of Malaita and Santa Isabel, Solomon
797 Islands, southern margin of Ontong Java Plateau. *J. Petrol.* 37, 361-394.
- 798 Tejada, M.L.G., Mahoney, J.J., Neal, C.R., Duncan, R.A., Petterson, M.G., 2002.
799 Basement geochemistry and geochronology of central Malaita, Solomon Islands,
800 with implications for the origin and evolution of the Ontong Java Plateau. *J. Petrol.*
801 43, 449-484.
- 802 Walker, R.J., Carlson, R.W., Shirey, S.B., Boyd, F.R., 1989. Os, Sr, Nd, and Pb isotope
803 systematics of southern African peridotite xenoliths: implications for the chemical
804 evolution of subcontinental mantle. *Geochim. Cosmochim. Acta* 53, 1583-1595.
- 805 Walker, R.J., Horan, M.F., Morgan, J.W., Becker, H., Grossman, J.N., Rubin, A.E., 2002.
806 Comparative ¹⁸⁷Re–¹⁸⁷Os systematics of chondrites: implications regarding early
807 solar system processes. *Geochim. Cosmochim. Acta* 66, 4187-4201.
- 808 Walker, R.J., Brandon, A.D., Bird, J.M., Piccoli, P.M., McDonough, W.F., Ash, R.D.,
809 2005. ¹⁸⁷Os–¹⁸⁶Os systematics of Os–Ir–Ru alloy grains from southwestern Oregon.
810 *Earth Planet. Sci. Lett.* 230, 211-226.
- 811 Widom, E., Hoernle, K.A., Shirey, S.B., Schmincke, H.-U., 1999. Os isotope
812 systematics in the Canary Islands and Madeira: lithospheric contamination and
813 mantle plume signatures. *J. Petrol.* 40, 279-296.
- 814 Workman, R.K., Hart, S.R., 2005. Major and trace element compositions of the depleted
815 MORB mantle (DMM). *Earth Planet. Sci. Lett.* 231, 53-72.

Figure captions

Fig. 1. Map of (A) present-day and (B) 35 Ma plate configurations of southeast Asia and the southwest Pacific after Hall (2002).

Fig. 2. (A) P - T estimates for Malaita peridotite and pyroxenite xenoliths based on Brey and Köhler (1990) thermobarometry. Thick dashed lines labelled as PSM and GDH1 represent the asymptotic geotherms for old oceanic lithosphere from Parsons and Sclater (1977) and Stein and Stein (1992), respectively. Solidus, liquidus and 30% melting contour (thin dashed line) for fertile peridotite and adiabatic gradients are taken from Herzberg (2004). The overall resemblance between P - T array of xenoliths (34 Ma Malaita geotherm) and the theoretical oceanic geotherms suggest that (1) ~90 m.y. of cooling since the Ontong Java Plateau magmatism to the time of the xenoliths entrainment was adequate for cooling of the lithosphere to a nearly steady-state; (2) the thermal perturbation accompanied by the host eruption was negligible probably because the alnöite (a silica-undersaturated ultramafic magma with affinities to kimberlite) is a very small degree partial melt. Filled ellipse indicates possible melting condition for generating an intra-lithospheric depleted zone estimated by assuming that (1) harzburgite containing Fo₉₂ olivine was residual after 30% melting of fertile peridotite and (2) subsequent cooling path to the 34 Ma Malaita geotherm was nearly isobaric. (B) Forsterite (Fo) contents in olivine from spinel lherzolites (filled circles), garnet lherzolites (open circles) and spinel harzburgites (grey circles) against estimated temperature. Corresponding depths are also shown in y axis. Dashed line is the boundary between high-temperature type and low-temperature type groups. The hatched field represents an intra-lithospheric depleted zone defined by lack of garnet-bearing xenoliths (see text for details). Histogram and probability density curve for all plots are also shown. A 'bandwidth' uncertainty for probability density curve was set to be identical to the width of histogram bin.

Fig. 3. Co-variation of (A) forsterite (Fo) content in olivine and (B) spinel Cr# $[=Cr/(Cr+Al)]$ with whole-rock Al_2O_3 content of low-T type (GSL: garnet-spinel lherzolite, SL: spinel lherzolite, SH: spinel harzburgite) and high-T type (GL: garnet lherzolite, SH: spinel harzburgite) groups of Malaita peridotite xenoliths. The estimates for primitive upper mantle (PUM) are indicated by open squares (McDonough and Sun, 1995). Shaded field encompasses global compilations of oceanic peridotites (shaded squares) including abyssal peridotites and oceanic peridotite xenoliths. Complete data sources are found in Simon et al. (2008).

Fig. 4. Histogram and probability density curve showing Re and Os concentrations for oceanic peridotites (A and C, respectively) and for Malaita peridotite xenoliths (B and D, respectively). Shaded bars in A and C are published data of abyssal peridotites (Liu et al., 2008), hatched bars are oceanic peridotite xenoliths (Hauri, 1992; Hassler and Shimizu, 1998; Widom et al., 1999; Meisel et al., 2001; Becker et al., 2006; Bizimis et al., 2007; Simon et al., 2008), respectively. Shaded bars in B and D are Malaita low-T peridotite xenoliths, hatched bars are high-T peridotite xenoliths (this study). An estimate for primitive upper mantle (PUM) is shown for comparison (Becker et al., 2006). A 'bandwidth' uncertainty for probability density curve was set to be identical to the width of histogram bin.

Fig. 5. Histogram and probability density curve showing measured $^{187}Os/^{188}Os$ ratios and T_{RD} ages for (A) chondrites (Walker et al., 2002), (B) abyssal peridotites (data sources as in Fig. 4.), (C) oceanic peridotite xenoliths (data sources as in Fig. 4.) and (D) Malaita peridotite xenoliths data (shaded: low-T peridotites, hatched: high-T peridotites). The estimate for the primitive upper mantle (PUM) is shown for comparison (Meisel et al., 2001). A 'bandwidth' uncertainty for probability density curve of 0.0025 was applied to the $^{187}Os/^{188}Os$ ratios of all samples.

Fig. 6. (A) Co-variation of measured $^{187}Os/^{188}Os$ ratios against $^{187}Re/^{188}Os$. Symbols and data sources are as in Figs. 3 and 4, respectively. Inset shows overall variations of low-T spinel harzburgites which can be divided into two subgroups: (1) a main group (n=14) yielding an apparent age of 111 ± 24 Ma (mean square weighted deviation=447)

with initial $^{187}\text{Os}/^{188}\text{Os}=0.1236\pm6$; (2) an unradiogenic group ($n=4$) yielding an apparent age of 129 ± 10 Ma (mean square weighted deviation=13) with initial $^{187}\text{Os}/^{188}\text{Os}=0.1163\pm5$. Dashed lines in the inset denote reference isochrons with ages of 122 Ma (Ontong Java Plateau magmatism) and 34 Ma (host alnöite eruption).

Fig. 7. Histogram and probability density curve showing (A) present-day $^{187}\text{Os}/^{188}\text{Os}$ ratios and $T_{\text{RD-122 Ma}}$ ages for platinum-group alloy grains (PGAs) derived from Jurassic-Cretaceous (90-165 Ma) ophiolites (Meibom et al., 2002; Pearson et al., 2007), (B, C, D) 122 Ma-corrected $^{187}\text{Os}/^{188}\text{Os}$ ratios and $T_{\text{RD-122 Ma}}$ ages for low-T peridotite and high-T peridotite xenoliths from Malaita (B and C, respectively) and peridotite xenoliths from Salt Lake Crater (SLC), Hawaii (D, Bizimis et al., 2007). Noted that Re-ingrowth correction for SLC xenoliths was not applied because recent metasomatism by a Hawaiian melt likely modified their bulk Re concentrations. The estimate for the 122 Ma primitive upper mantle (PUM) is shown for comparison (Meisel et al., 2001). A ‘bandwidth’ uncertainty for probability density curve of 0.0025 was applied to the $^{187}\text{Os}/^{188}\text{Os}$ ratios of all samples.

Fig. 8. Co-variation of (A) Os concentrations [ppb and normalised to primitive upper mantle (PUM: Becker et al., 2006)] and (B) 122 Ma-corrected $^{187}\text{Os}/^{188}\text{Os}$ ratios and $T_{\text{RD-122 Ma}}$ ages with estimated temperatures (Ishikawa et al., 2004) of Malaita peridotites. Symbols are as in Figs 3. (C, D) Inferred stratigraphic succession beneath the Ontong Java Plateau at 34 Ma (C) and at 122 Ma just before the plateau emplacement (D).

Fig. S1. Co-variation of 122 Ma-corrected $^{187}\text{Os}/^{188}\text{Os}$ ratios against (A) whole-rock LOI content, (B) whole-rock Al_2O_3 content, (C) forsterite (Fo) content in olivine and (D) spinel Cr# [$=\text{Cr}/(\text{Cr}+\text{Al})$]. Dotted tie-lines connect 122 Ma-corrected and present-day ratios shown by transparent symbols. Symbols and data sources are as in Figs 3 and 4, respectively.

Table 1 Footnote

GL: garnet lherzolite, SH: spinel harzburgite, GSL: garnet-spinel lherzolite, SL: spinel lherzolite, SH: spinel harzburgite; dupl., duplicate analyses of Re-Os isotopes; P - T estimates and mineral data (Fo in olivine and Cr# in spinel) from Ishikawa et al. (2004);

912 Pressure values in brackets were obtained as the intersection of the geotherm (a linear
 913 regression of the P - T array) with estimated temperatures; Uncertainties on measured
 914 isotope ratios (given in brackets) are $2\sigma_{\text{mean}}$; $^{187}\text{Os}/^{188}\text{Os}$ ratios normalised using
 915 $^{192}\text{Os}/^{188}\text{Os}=3.08271$ and corrected using $^{18}\text{O}/^{16}\text{O}$ and $^{17}\text{O}/^{16}\text{O}$ of 0.002045 and
 916 0.000371 respectively; Average total procedural blanks were 1.1 and 1.7 pg for Re and
 917 Os, respectively, with a $^{187}\text{Os}/^{188}\text{Os}$ ratio of 0.150. Blank corrections relate to the
 918 appropriate reagent batch rather than a long-term mean, but their contributions to
 919 measured Re and Os concentrations and $^{187}\text{Os}/^{188}\text{Os}$ ratios were typically less than 10%,
 920 0.2% and 0.1%, respectively; contributions for some low abundance samples were
 921 greater (<30%, <7% and <0.7%, respectively); T_{RD} ages (Ga) are calculated by using
 922 present-day $^{187}\text{Os}/^{188}\text{Os}$ ratios relative to the evolution of average chondrite
 923 ($^{187}\text{Os}/^{188}\text{Os}=0.1276$), whereas $T_{\text{RD-122 Ma}}$ ages (Ga) are calculated by using
 924 $^{187}\text{Os}/^{188}\text{Os}_{122 \text{ Ma}}$ relative to the evolution of PGAs from Mesozoic ophiolites
 925 ($^{187}\text{Os}/^{188}\text{Os}_{122 \text{ Ma}}=0.1251$), respectively (see text for details).

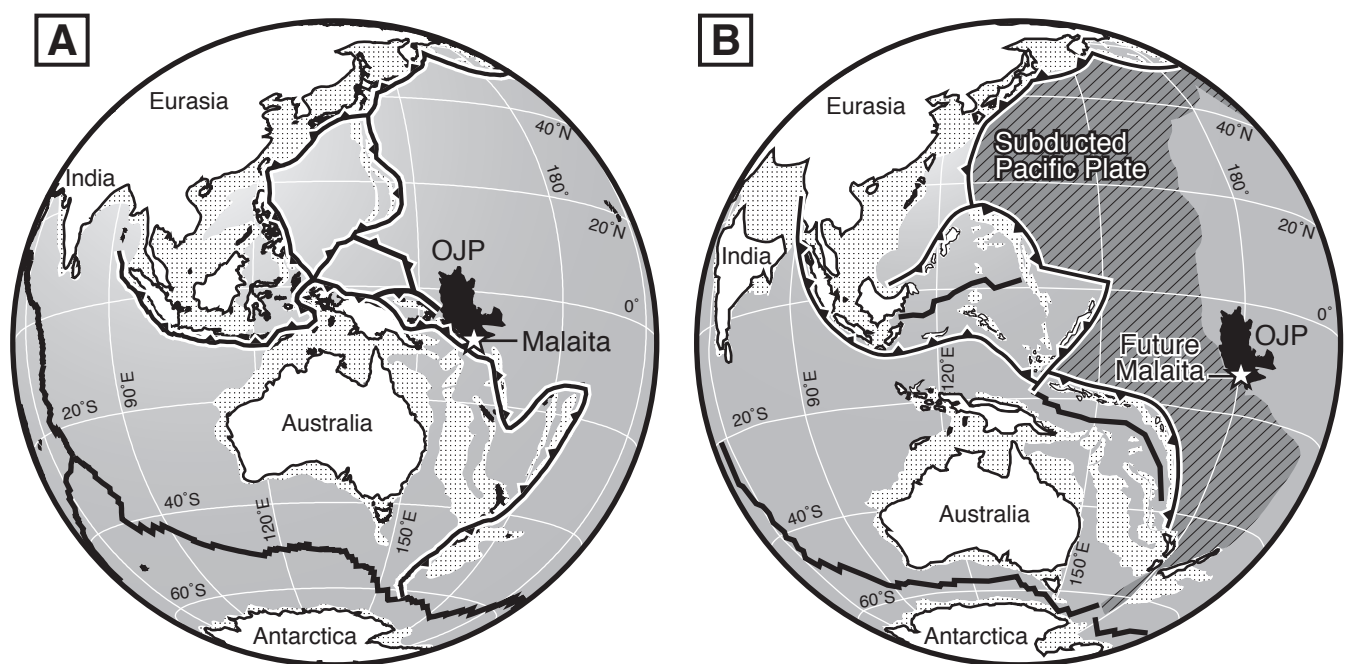


Fig. 1. A. Ishikawa et al. / submitted to Earth and Planetary Science Letters

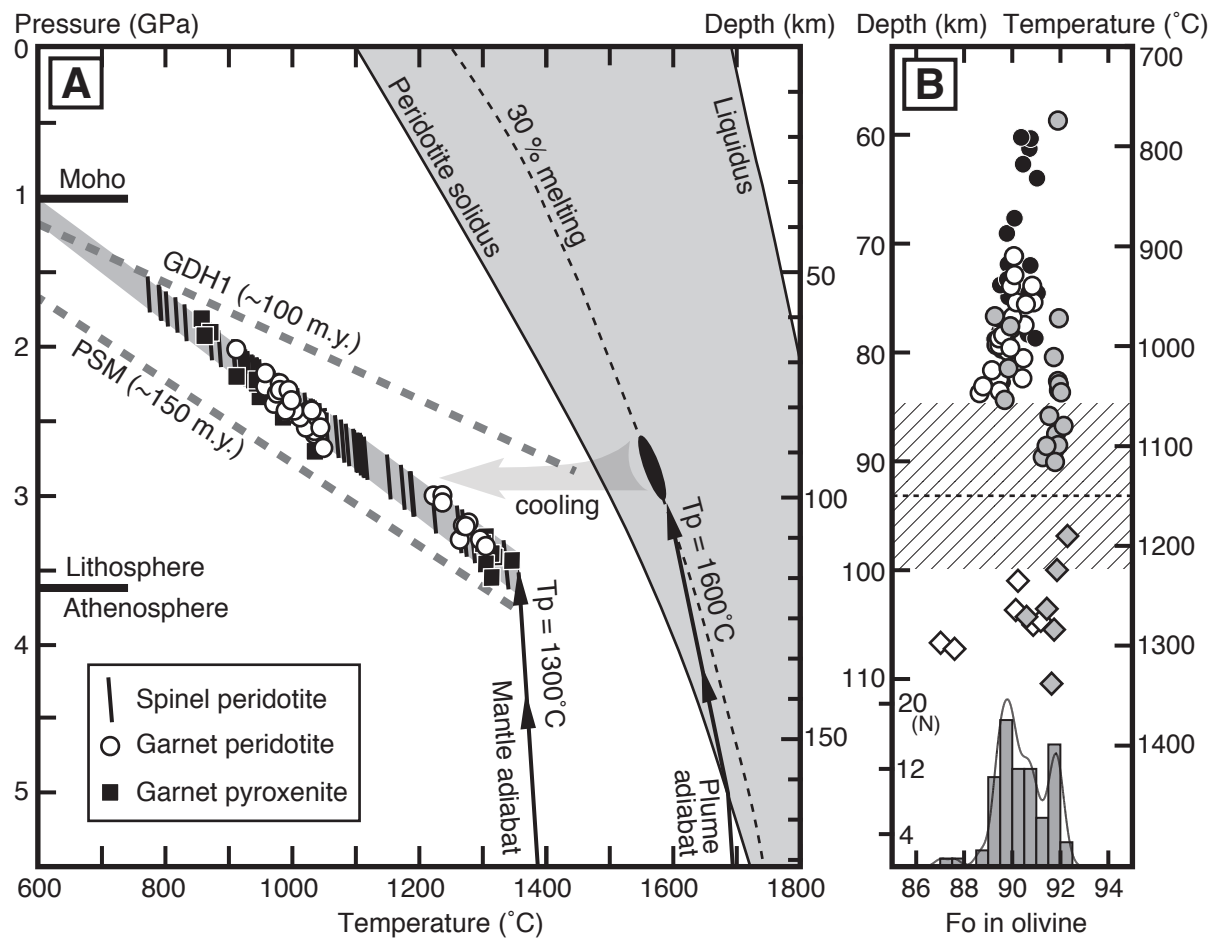


Fig. 2. A. Ishikawa et al. / submitted to Earth and Planetary Science Letters

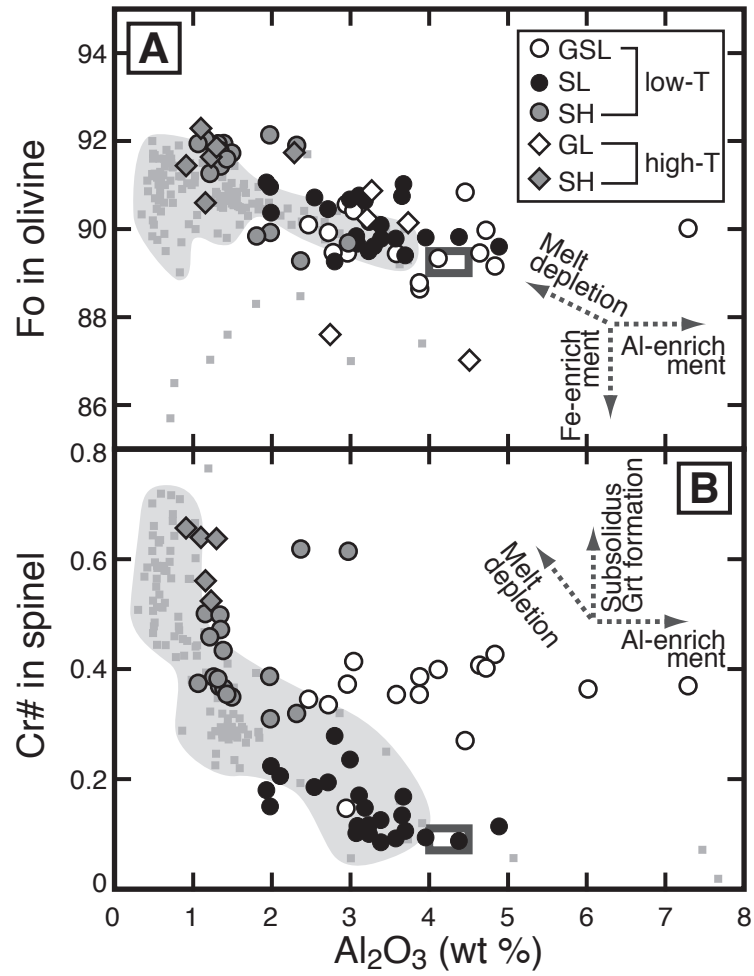


Fig. 3. A. Ishikawa et al. / submitted to Earth and Planetary Science Letters

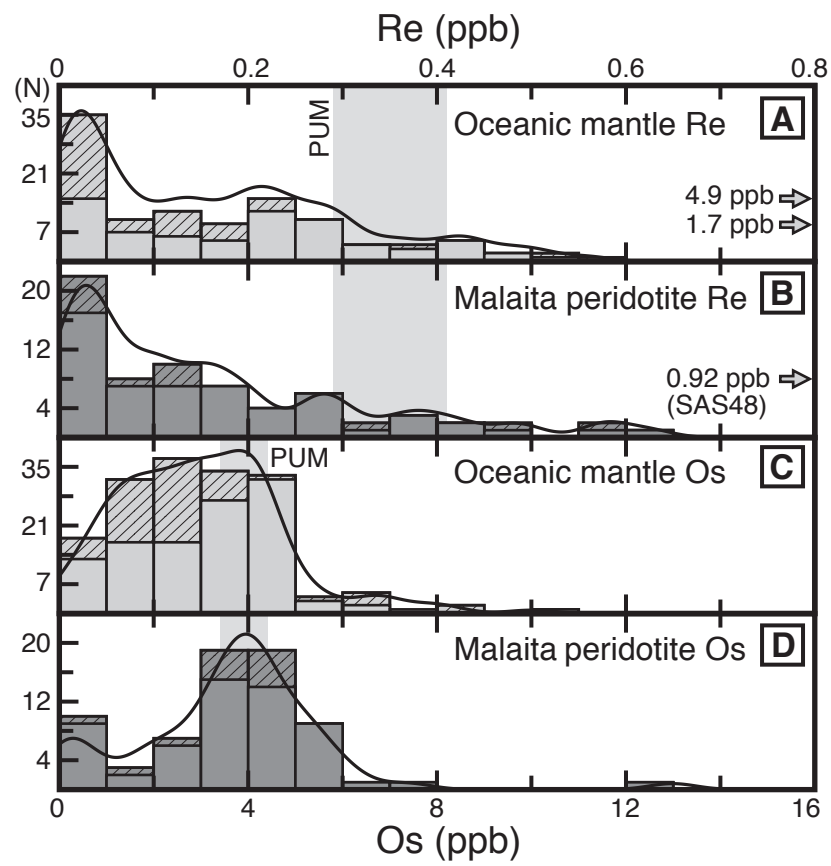


Fig.4 . A. Ishikawa et al. / submitted to Earth and Planetary Science Letters

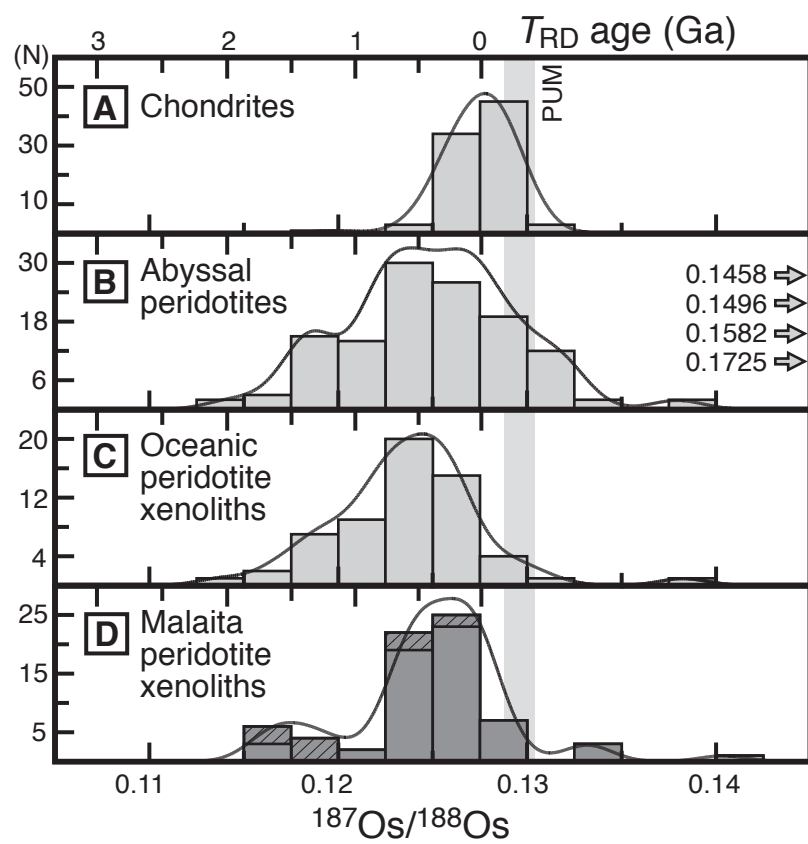


Fig. 5. A. Ishikawa et al. / submitted to Earth and Planetary Science Letters

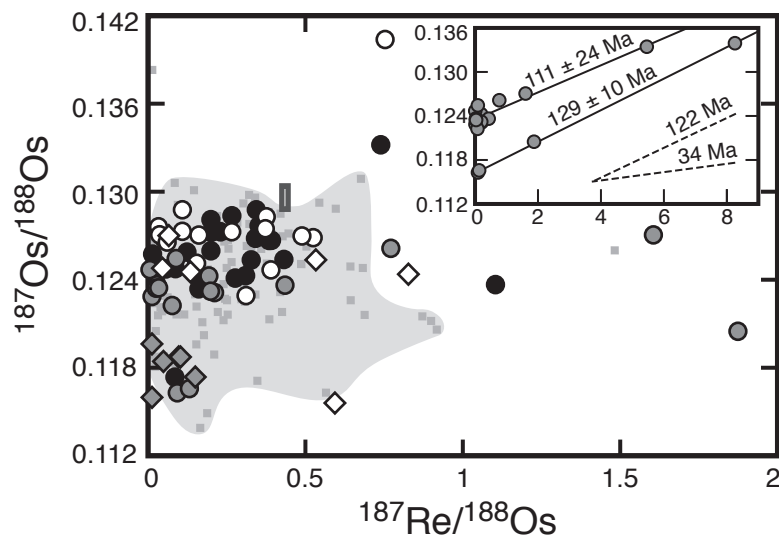


Fig. 6. A. Ishikawa et al. / submitted to Earth and Planetary Science Letters

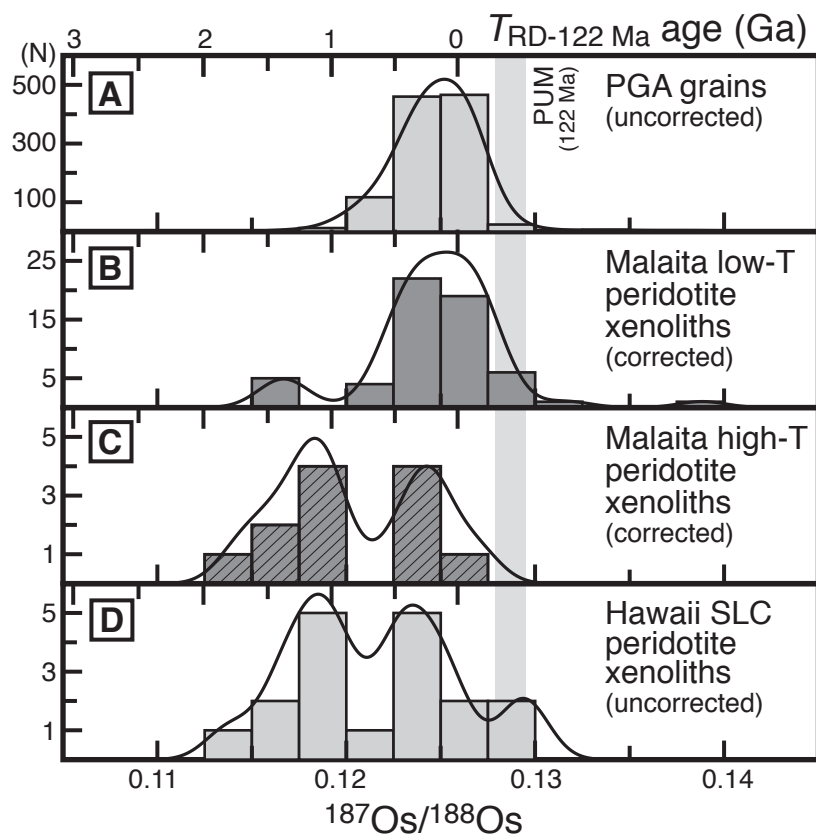


Fig. 7. A. Ishikawa et al. / submitted to Earth and Planetary Science Letters

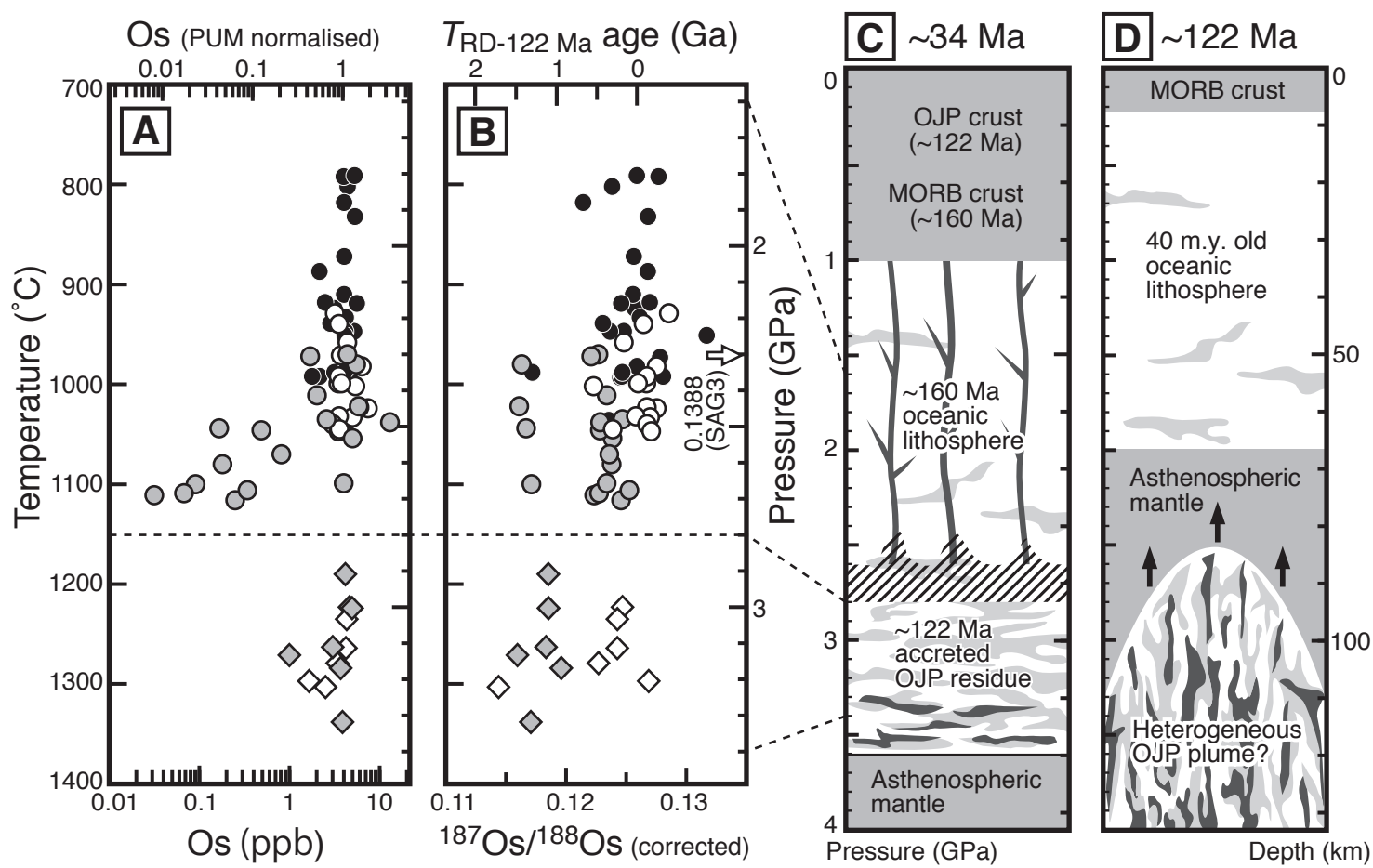


Fig. 8. A. Ishikawa et al. / submitted to Earth and Planetary Science Letters